Conformations of Arg-Gly-Asp Containing Heterodetic Cyclic Peptides: Solution and Crystal Studies

Kenneth D. Kopple,* Paul W. Baures, John W. Bean, Cynthia A. D'Ambrosio, John L. Hughes,† Catherine E. Peishoff, and Drake S. Eggleston

Contribution from the Department of Physical and Structural Chemistry, UW 2940, SmithKline Beecham Pharmaceuticals, P.O. Box 1539, King of Prussia, Pennsylvania 19406.
Received April 29, 1992

Abstract: Peptides containing the sequence Arg-Gly-Asp antagonize binding of fibrinogen to its platelet GPIIb/IIIa receptor, thereby inhibiting platelet aggregation. Incorporation of the sequence into cyclic pentapeptide disulfides has been reported to yield effective antagonists. The conformations in solution of two such antagonists, (2-mercaptobenzoyl)-N^{α}-methylArg-Gly-Asp-2-mercaptoanilide cyclic disulfide (**1**) and Ac-Cys-N^{α}-methylArg-Gly-Asp-Pen-NH_2 cyclic disulfide (**2**), have been studied using a constrained distance geometry search procedure in conjunction with proton NMR data, and a structure of **1** has been determined from single-crystal X-ray diffraction data. NMR spectra of the cyclic diaryl disulfide **1** at 203 K in methanol show two slowly exchanging conformations. The Arg-Gly-Asp region of the major form is characterized, inter alia, by an extended Gly residue flanked by an N^{α}-methylArg residue in a conformation roughly consistent with the $i + 2$ position of a β-turn and an Asp residue in a C_7 like conformation. In the minor component, the Asp residue is near the α_R conformation. The barrier to exchange between the two forms is estimated at 11 kcal/mol. NMR data and analysis of the constrained distance geometry search results suggest that, at room temperature in dimethyl sulfoxide–sulfolane, the dominant conformation of the Arg-Gly-Asp regions of both **1** and **2** is like that in the major component of **1** at 203 K. (2-Mercaptobenzoyl)-N^{α}-methyl-Arg-Gly-Asp-2-mercaptoanilide cyclic disulfide (**1**) was crystallized from aqueous ethanol as a solvated nitrate salt in a cell of dimensions $a = 27.919$ (16) Å, $b = 7.552$ (3) Å, $c = 16.3131$ (10) Å, and $\beta = 108.79$ (5)° with four formula units in space group $C2$. The structure was solved by direct methods and refined to $R = 0.057$ for 2869 observations ($I \geq 3\sigma(I)$). The crystal structure of **1** and the most probable conformation of its minor form in solution agree closely.

Introduction

The development of agents which inhibit cell to cell adhesion processes is an important area of antithrombotic research. It has been shown that platelet aggregation is dependent on the interaction of fibrinogen with the platelet GPIIb/IIIa receptor and that the smallest protein fragment to bind the receptor is the tetrapeptide Arg-Gly-Asp-Ser.[1-3] This short sequence provides an opportunity to use conformationally restricted analogs to derive information about the receptor-bound conformation of a biologically active peptide. Previous reports from these laboratories have described a series of cyclic disulfide fibrinogen receptor antagonists, including two highly active, and to some extent conformationally restricted, inhibitors of platelet aggregation: (2-mercaptobenzoyl)-N^{α}-methylArg-Gly-Asp-2-mercaptoanilide cyclic disulfide (**1**)[4] and Ac-Cys-N^{α}-methylArg-Gly-Asp-Pen-NH_2 cyclic disulfide (**2**).[5]

We report here nuclear magnetic resonance and X-ray crystallographic studies of these two compounds. NMR-based conformational studies, using distance geometry search methods,[6-8] have been carried out on both **1** and **2**, including a study of the diaryl disulfide analog **1** at 203 K in which two slowly exchanging conformations were characterized. A crystal structure of **1** has been determined, and a probable conformation for one of the slowly exchanging conformations corresponds to it. The results of these studies show that although these heterodetic cyclic peptides are not rigid, they share a probable conformation of the Arg-Gly-Asp sequence that is characterized by an extended conformation of the Gly residue.

Methods

NMR Measurements. Proton NMR data were collected by employing a Bruker AMX500 spectrometer and processed using the program package FELIX (Hare Research, Woodinville, WA). Dimethyl-d_6 sulfoxide (DMSO-d_6) (99.96%), tetramethylene-d_8 sulfone (sulfolane-d_8) (98.5%), methanol-d_3 (99.8%), and methanol-d_4 (99.96%) were obtained from MSD Isotopes, Montreal, Canada. Proton chemical shift assignments were made by standard procedures using DQF-COSY, P.E.COSY,[9] TOCSY, and NOESY spectra. Peptides were examined as trifluoroacetate salts at 3–5 mM concentration. Coupling constants were measured from P.E.COSY or 1-D spectra. Chemical shifts and coupling constants are reported in Tables I and II. For both **1** and **2** in 5:3 DMSO–sulfolane at 303 K, NOESY crosspeaks were integrated in spectra measured at mixing times of 50, 100, 150, and 200 ms. For **1** in methanol-d_3 at 203 K, mixing times of 50, 100, and 150 ms were used.

Interproton distances were calculated from the buildup rates of the crosspeak volumes. Buildup rates were obtained by least squares fitting of the measured points. Rates for which the linear fit gave correlation coefficients greater than 0.9 were used to determine distance constraints that were assigned both upper and lower bounds in the distance geometry calculations, subsequently referred to as doubly-bounded constraints. For **1**, the mean of the initial buildup rates of well-resolved NOE crosspeaks involving vicinal aromatic ring protons was used as a distance reference corresponding to 2.49 Å. For **2**, the mean of the buildup rates of Gly $H^{\alpha 1}$–$H^{\alpha 2}$ crosspeaks, taken as corresponding to 1.75 Å, was used for proton–proton distances. For proton–methyl distances in **2**, the mean of the buildup rates for the Cys H^N–acetyl CH_3 crosspeaks was used. A centroid (1.02 Å from each of the methyl protons and 0.4 Å from the methyl carbon) was used as the position of the methyl group; with this centroid, the Cys H^N–acetyl CH_3 reference distance is 2.92 Å. Further specifics are given with the distance constraints in Table III. Penalty-free upper and lower bounds for the distance geometry calculations were taken as −10% and +15% of the distance calculated from the reference volumes.

* Author to whom correspondence should be addressed.
† Department of Synthetic Chemistry.

(1) Gartner, T. K.; Bennett, J. S. *J. Biol. Chem.* **1985**, *260*, 11891–11894.
(2) Lam, S. C.-T.; Plow, E. F.; Smith, M. A.; Andrieux, A.; Ryckwaert, J.-J.; Marguerie, G.; Ginsberg, M. H. *J. Biol. Chem.* **1987**, *262*, 947–950.
(3) Plow, E. F.; Pierschbacher, M. D.; Ruoslahti, E.; Marguerie, G.; Ginsberg, M. H. *Blood* **1987**, *70*, 110–115.
(4) Ali, F. E.; Samanen, J. M.; Calvo, R.; Romoff, T.; Yellin, T.; Vasko, J.; Powers, D.; Stadel, J.; Bennett, D.; Berry, D.; Nichols, A. In *Peptides: Chemistry and Biology, Proceedings of the Twelfth American Peptide Symposium*; Smith, J. A., Rivier, J. E., Eds.; ESCOM Science Publishers B.V.: Leiden, The Netherlands, 1992; pp 761–762.
(5) Samanen, J.; Ali, F.; Romoff, T.; Calvo, R.; Sorenson, E.; Vasko, J.; Storer, B.; Berry, D.; Bennett, D.; Strohsacker, M.; Powers, D.; Stadel, J.; Nichols, A. *J. Med. Chem.* **1991**, *34*, 3114–3125.
(6) Bean, J. W.; Kopple, K. D.; Peishoff, C. E. *J. Am. Chem. Soc.* **1992**, *114*, 5328–5334.
(7) Peishoff, C. E.; Bean, J. W.; Kopple, K. D. *J. Am. Chem. Soc.* **1991**, *113*, 4416–4421.
(8) Peishoff, C. E.; Dixon, J. S.; Kopple, K. D. *Biopolymers* **1990**, *30*, 45–56.
(9) Mueller, L. *J. Magn. Reson.* **1987**, *72*, 191–196.

0002-7863/92/1514-9615$03.00/0

Table I. Chemical Shifts and Coupling Constants for (2-Mercaptobenzoyl)N^{α}-MeArg-Gly-Asp-2-mercaptoanilide Cyclic Disulfide (**1**) in Methanol at 203 K and in 5:3 DMSO–Sulfolane at 303 K

residue	H^N ($H^{N\text{-}Me}$), ppm	H^{α}, ppm	H^{β}, ppm	H^{γ}, ppm	H^{δ}, ppm	$J(H^N\text{–}H^{\alpha})$, Hz	$J(H^{\alpha}\text{–}H^{\beta})$, Hz
Arg							
203 K, major	(2.01)	5.25	1.67/1.45	1.47	3.11		
203 K, minor	(2.68)	5.36	1.90/1.59	1.59	3.19		
303 K	(2.25)	5.22	1.73/1.66	1.43	3.13		
Gly							
203 K, major	9.25	3.96/3.59				5.0/6.3	
203 K, minor	9.17	3.96/3.72				5.7/?	
303 K	8.17[b]	4.03/3.58					
Asp							
203 K, major	9.57	4.99	3.05/2.75			6.0	7.5/7.5
203 K, minor	9.48	4.81	3.02/2.92			6.0	
303 K	9.00[b]	4.84	2.90/2.62				

	H^N	H3	H4	H5	H6
Mba[a]					
203 K, major		8.26	7.61	7.36	7.15
203 K, minor		7.91	7.53	7.47	7.30
303 K		8.05	7.57	7.38	7.18
Man[a]					
203 K, major	9.96	7.51	6.98	7.38	7.95
203 K, minor	9.55	7.66	7.26	7.31	7.50
303 K	9.52[b]	7.66	7.06	7.41	8.08

[a] Abbreviations: Mba, 2-mercaptobenzoic acid; Man, 2-mercaptoaniline. [b] H^N chemical shift temperature coefficients in ppm deg^{-1}: Gly, 0.0013; Asp, 0.0059; Man 0.0033.

Table II. Proton Chemical Shifts of Ac-Cys-N^{α}-MeArg-Gly-Asp-Pen-NH_2 Cyclic Disulfide (**2**) in 5:3 DMSO-d_6–Sulfolane-d_8 at 303 K

residue	H^N, ppm	$d\delta/dT$[b]	H^{α}, ppm	H^{β}, ppm	H^{γ}, ppm	H^{δ}, ppm	other, ppm	$J(H^N\text{–}H^{\alpha})$, Hz
Cys	8.30	0.0068	4.89	3.05, 2.96			CH_3CO, 1.88	
N-MeArg	2.99 (Me)		4.99	1.81, 1.64	1.42, 1.39	3.13	HN[c], 7.57	
Gly	7.30	0.0037	4.15, 3.39					7.3, 3.6
Asp	8.13	0.0046	4.16	2.71, 2.54				7.4
Pen	7.71	0.0044	4.38	1.38			H_2N, 7.50, 7.07	8.5

[a] From P.E.COSY spectrum. [b] H^N chemical shift temperature coefficients in ppm deg^{-1}.

The NOE data were selected and utilized substantially as described earlier.[6] Only data for peptide backbone, aromatic, and *N*-methyl protons were used to determine the doubly-bounded constraints. Potential interproton interactions that did not give rise to observed Overhauser crosspeaks at the longest mixing time were used to provide lower bound only, or anti, distance constraints (ADC's).[6,10] ADC's, set at 3.0 Å, were assigned to interproton distances for all H^{α}, H^N, and H^{β} interproton distances if no crosspeak was observed in the column and row slices containing the corresponding resonances. Sensitivity was such that, for **1** in methanol at 203 K, for example, the signal to noise ratio (S/N) at 150-ms mixing time for a crosspeak from the major component (of two in slow exchange) corresponding to a 3.23-Å calculated distance was 23 and, for one from the minor component corresponding to 3.37 Å, S/N was 7. In cases of chemical shift overlap, including overlap with exchange crosspeaks, neither a doubly-bounded distance constraint nor an ADC was assigned. Interproton distances were also omitted between protons with covalently determined fixed distances, i.e., aromatic ring protons. An ADC was also not assigned if a signal with intensity corresponding to a distance shorter than 3.5 Å was observed in any row or column common to that crosspeak. In one instance, noted in Table III, an upper bound only constraint was applied.

Conformation Searches.[6,7] Conformations were generated for compounds **1** and **2** using the program DGEOM (available from QCPE, Department of Chemistry, Indiana University, Bloomington, IN 47405). Torsion sampling was applied, distance correlation was turned off, and 500 conformers were generated during each run.[8] All nonaromatic bonds were considered fully rotatable with the exception of amide bonds, which were allowed to be either cis or trans. The NOE data were applied in the following manner. For compound **1**, 303 K data included 8 doubly-bounded constraints and 193 ADC's. For compound **1**, 203 K, major conformer data included 10 doubly-bounded constraints and 150 ADC's. For compound **1**, 203 K, minor conformer data included 7 distance constraints and 176 ADC's. For compound **2**, 303 K data included 9 distance constraints, 200 ADC's, and, for 1 observed NOE which was difficult to integrate, an upper-bound value of 3.5 Å. (See Table III, note *g*) For compound **2**, a pseudoatom was placed 0.4 Å from carbon and

Table III. Overhauser Effect Based Distance Constraints for (2-Mercaptobenzoyl)-N^{α}-MeArg-Gly-Asp-2-mercaptoanilide Cyclic Disulfide (**1**) and Ac-Cys-N^{α}-MeArg-Gly-Asp-Pen-NH_2 Cyclic Disulfide (**2**)

		calculated interproton distances, Å			
		methanol, 203 K		DMSO–sulfolane,[a] 303 K	
proton 1	proton 2	**1**, major[b]	**1**, minor[c]	**1**[d]	**2**[e]
Mba 3	Man 3	2.61	2.56		
Cys α	Arg *N*-Me[f]				<3.50[g]
Arg *N*-Me[f]	Arg α				>3.00[j]
Arg *N*-Me[f]	Gly N				>3.00[j]
Arg α	Gly N	2.42	2.96	2.64	2.36
Gly N	Gly α1	2.60	2.86	3.01	2.50
Gly N	Gly α2	2.59	3.26[h]	2.70	2.48
Gly α1	Asp N	2.54	2.53	2.27	2.44
Gly α2	Asp N	2.60	3.37	2.87	2.68
Asp N	Asp α	2.86	>3.00[i]	2.89	2.66
Asp N	Man N	3.23		3.18	
Asp N	Pen N				>3.00[j]
Asp α	Man N	2.48	3.61	2.45	
Asp α	Pen N				2.32
Man N	Man 6	3.13			
Pen N	Pen α				2.61

[a] 5:3 DMSO-d_6–sulfolane-d_8. [b] Reference crosspeaks: vicinal aromatic protons, mean volume buildup rate of 10 ≡ 2.49 Å, range 2.38–2.63 Å. [c] Reference crosspeaks: vicinal aromatic protons, mean volume buildup rate of 2 ≡ 2.49 Å, range 2.47–2.51 Å. [d] Reference crosspeaks: vicinal aromatic protons, mean volume buildup rate of 2 ≡ 2.49 Å, range 2.46–2.51 Å. [f] *N*-methyl group centroid. [g] Assigned upper bound. This crosspeak yielded a calculated distance of 2.43 Å and was of greater intensity than either of the adjacent Cys H^{α}–H^{β} peaks. It was not used quantitatively because it overlapped them. [h] This calculated value is larger than the geometric limit (2.98 Å); however, the penalty-free range overlaps the geometrically permissible range. [i] Observed with intensities corresponding to about 3.5 Å; but not used as a constraint because of a correlation coefficient <0.9. [j] Standard ADC; however, see discussion of **2** in Results.

(10) Brüschweiler, R.; Blackledge, M.; Ernst, R. R. *J. Biomol. NMR* **1991**, *1*, 3–11.

Table IV. Probable Solution Conformations of (2-Mercaptobenzoyl)-N^{α}-MeArg-Gly-Asp-2-mercaptoanilide Cyclic Disulfide (**1**)[a]

			N-MeArg		Gly		Asp		Man[c]		-S-S-[c]	Mba[c]	
class	E_{total}[b], kcal mol^{-1}	E_{constr}, kcal mol^{-1}	ϕ, deg	ψ, deg	ϕ, deg	ψ, deg	ϕ, deg	ψ, deg	C16-N17-C18-C23	S1-S2-C23-C18	C6-S1-S2-C23	S2-S1-C6-C1	C6-C1-C7-N8
Major Component, Methanol, 203 K													
1A+	15.13	0.03	**-105**	**60**	**175**	**-160**	**-86**	**79**	99	**75**	**104**	**87**	**-116**
1A-	16.53	0.18	**-123**	**73**	**-175**	**-149**	-79	79	**108**	**-108**	**-95**	**-67**	**-67**
1B+	17.47	0.73	-99	65	82	154	53	60	87	119	107	66	-131
1B-	18.58	0.77	-88	80	90	152	59	67	91	-90	-108	-90	-111
Minor Component, Methanol, 203 K													
1C+	15.39	0.21	**-94**	**56**	**178**	**-147**	**-76**	**-57**	**-86**	95	**101**	**73**	**-125**
1C-	15.51	0.05	-112	56	-166	-145	-67	-46	-87	79	-97	-91	-80
1D+	15.31	0.04	-101	58	-163	-86	-153	-59	-90	85	113	95	-127
1D-	16.22	0.04	-130	59	-157	-90	-122	-58	-78	-76	-94	-91	-67
DMSO-Sulfolane, 303 K[d]													
	14.63	0.02	-117	61	176	-158	-87	67	99	72	98	100	-95
Crystal Structure													
			-119	**69**	**-178**	**-164**	**-61**	**-33**	**-128**	98	**102**	**99**	**-98**

[a] Lowest energy conformations of each class returned by the constrained distance geometry searches. The dihedral angles of 1A±, 1C+, and the crystal structure are in boldface for ease of comparison. [b] Energy calculated using AMBER 3.0. [c] Numbering for dihedral angles (deg) is given as for the X-ray structure. See Figure 4. [d] Lowest energy conformation found using data from 5:3 DMSO-sulfolane solution at 303 K.

1.02 Å from each hydrogen of the N^{α}-methyl group on Arg and used as the constraint atom for this group. The doubly-bounded constraints for each run are listed in Table III.

Each conformer was minimized using the program AMBER 3.0[11] modified to accept distance bounds. All partial charges were set to zero to eliminate electrostatic energy terms. Conformers were minimized until the norm of the gradient of the energy reached 0.01 kcal mol^{-1} Å^{-1}. The NMR derived distance constraints were applied using a flat-bottomed well potential with harmonic sides such that no penalty was assessed for distances falling within the bounds. A force constant of 50 kcal mol^{-1} Å^{-2} was used for each NMR-derived constraint. A force constant of 100 kcal mol^{-1} Å^{-2} was used to hold the pseudoatom in place. Modifications to the AMBER parameter set to allow for the aromatic residues included the following: CA-S = 1.79 Å; CA-N = 1.45 Å, angles, including CA, anilide N, and S, were approximated to closest counterpart in the AMBER dataset; dihedrals involving sulfur were given no rotation barrier; CA-N dihedral was given a 2-fold rotation barrier with a height of 3 kcal; and LP-S-LP were triangulated as previously described.[8]

Conformers with a maximum violation energy of 1.5 kcal, and with total energy no more than 5 kcal above the conformer of lowest total energy that met the 1.5 kcal condition, were classified on the basis of the backbone dihedral angles of the *N*-MeArg (N^{α}-methylarginine residue), Gly, and Asp residues. These clustered in groups of area ca. ±30° in the Φ-Ψ plane. Further specification of -S-S- chirality completed the definition of conformational classes. All conformations chosen under these energy criteria contained undistorted peptide bonds.

X-ray Diffraction of 1. Crystals of the nitrate salt of **1** were grown by slow evaporation from aqueous ethanol. The crystals obtained were inevitably small needles and diffracted weakly at best. The specimen used for data collection had approximate dimensions of 0.10 × 0.10 × 0.20 mm. The crystal was mounted on a glass fiber, coated with Paratone N oil, and flash frozen in a cold stream of nitrogen gas at 173 K. Lattice parameters were determined from the setting angles of 25 reflections located from a rotation photograph taken on an Enraf Nonius CAD4 diffractometer mounted on a GX-21 rotating anode equipped with graphite-monochromated copper radiation (λ(Kα) = 1.541 84 Å). The space group is *C*2 with a = 27.919 (16) Å, b = 7.652 (3) Å, c = 16.313 (10) Å, β = 108.79 (5)°, V = 3299 (2) Å^3, Z = 4, d_{calc} = 1.467 g cm^{-1} based on M_r = 728.81 for $(C_{26}H_{32}N_7O_6S_2)^+ \cdot (NO_3)^- \cdot H_2O \cdot C_2H_6O$, μ = 20.355 cm^{-1}, $F(000)$ = 1536. Data were measured on the diffractometer using an ω-2θ scan mode with a variable scan rate up to 7 deg min^{-1}, 2θ max = 135°, and index ranges $0 \le h \le 33$, $0 \le k \le 9$, and $-19 \le l \le 19$. Intensities (3305 collected) were corrected for Lorentz and polarization effects. The intensities of three standards measured every 3 h of exposure time showed a systematic increase for which a correction was applied to the values of F_{obs} (0.952 min, 1.000 max). Symmetry equivalent data were averaged (R_{int} = 0.032) to give a final set of 3231 observations. Of the latter, 2869 were considered observed with $I \ge 3\sigma(I)$. Data were also corrected for absorption, using the DIFABS procedure.[12] Correction factors ranged from 0.9300 min to 1.1572 max.

The structure was solved with SHELXS.[13] The y coordinate of atom S1 was held fixed to define the origin. Subsequent analysis showed the presence of a solvent channel containing somewhat poorly ordered electron density which was modeled eventually as containing a full occupancy water molecule and a molecule of ethanol occupying two overlapping orientations. An additional disorder, in the aspartyl carboxylic acid moiety, was evident from the difference maps. A two-site disorder model was incorporated for atoms C33, O34, and O35 at occupancies of 60% and 40%, as suggested from heights in a difference map and refinement of occupancy factors. These atoms were treated with isotropic temperature factors in the subsequent full-matrix least squares refinement. (There may be additional disorder in the nitrate anion, but a satisfactory model could not be worked out. The extensive disordering observed in this structure may be an artifact caused by flash freezing the crystal; none of it detracts from the conclusions of major interest with regard to the peptide conformation.) All other non-hydrogen atoms were refined with anisotropic displacement parameters. Occupancies for solvent atoms were refined initially to convergence and then fixed at coherent values to fit the model. Positions for many hydrogen atoms were suggested from difference Fourier maps. For the final model, hydrogens attached to carbons were fixed at calculated positions based on geometrical considerations and assigned isotropic temperature factors as 1.3 B_{eq} of the atom to which they are attached. Positions for hydrogen atoms attached to heteroatoms were assigned on the basis of considerations of hydrogen bonding interactions and also were held fixed with fixed isotropic temperature factors. The function minimized in least squares was $\sum w(|F_o| - |F_c|)^2$ with the weights, w, defined as $4F_o^2/\sigma(F_o^2)$ and $\sigma(F_o^2) = (\sigma^2(I_c) + (0.0016I^2))$. Final crystallographic residuals were R = 0.057, R_w = 0.075, and gof = 2.275 for a refinement of 447 variables. The refinement converged (max Δ/σ = 0.08). Maximum excursions in a final difference Fourier map were within ±0.783 e Å^{-3}. Neutral atom scattering factors from the International Tables for X-ray Crystallography[14] were used. Fractional coordinates for all atoms are available as supplementary material. Principal torsion angles for the backbone are listed in Table IV. Tables containing additional metrical details have been included with the deposited supplementary material.

Results

Solution Conformations of 1. (2-mercaptobenzoyl)-N^{α}-methylArg-Gly-Asp-2-mercaptoanilide cyclic disulfide (**1**) gives single-component spectra at room temperature in methanol or DMSO-sulfolane, but conformational exchange is indicated by the broader than expected *N*-MeArg H$^{\alpha}$ and *N*-MeArg *N*-CH$_3$ resonances at room temperature in both solvents and by differential line broadening below room temperature in methanol. At 203 K in methanol, the spectra of two components in slow exchange are well delineated, and spectral data and Overhauser enhance-

(11) Weiner, S. J.; Kollman, P. A.; Nguyen, D. T.; Case, D. A. *J. Comput. Chem.* **1986**, *7*, 230-252.

(12) Walker, N.; Stuart, D. *Acta Crystallogr.* **1983**, *A39*, 158-166.

(13) Sheldrick, G. M. In *Crystallographic Computing 3*; Sheldrick, G. M., Kruger, C., Goddard, R., Eds.; Oxford University Press: London, 1985; pp 175-189.

(14) Cromer, D. T. In *International Tables for X-ray Crystallography*; Kynoch Press (present distributor, D. Reidel, Dordrecht, The Netherlands): Birmingham, U.K., 1984; Vol. IV.

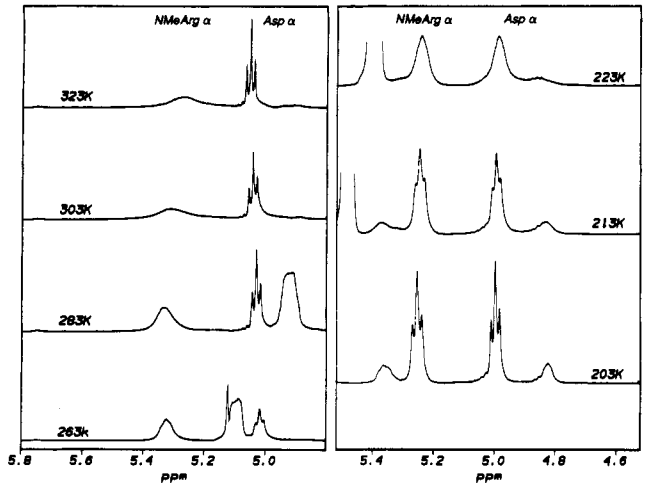

Figure 1. α-Proton resonances of N^{α}-methylArg and Asp residues of **1** in methanol-d_4 at indicated temperatures. The temperature dependence is discussed in the text.

ments for each may be extracted. Table I reports the chemical shift assignments for both components of **1** in methanol at 203 K and those obtained from the observed spectrum of **1** in DMSO–sulfolane at room temperature.

Figure 1 shows the *N*-MeArg α-proton and Asp α-proton resonances of **1** in methanol-d_4 at temperatures between 323 and 203 K. The line width of the *N*-MeArg H^{α} resonance exhibits biphasic behavior, showing a minimum near 263 K. The broadening of this signal above 263 K probably indicates the onset of exchange between cis and trans configurations of the benzoyl-N^{α}-methylArg peptide bond. Although cis–trans isomerization of N-alkylated peptide bonds more commonly becomes visibly significant on the chemical shift time scale only above room temperature, it may be that, in this aroyl case, line broadening occurs at a lower exchange rate because of a larger than usual chemical shift difference for the observed proton in the two states. No resonances that would correspond to the other component involved in this exchange are observed at any temperature, indicating a low fractional population.

For the exchange process with the lower energy barrier, the line shapes of the Asp α-proton resonances at 223, 213, and 203 K were simulated[15] to obtain an estimate of the exchange rates between the two states that are observed at those temperatures. The results for the three temperatures were consistent with a 4:1 ratio of two components and with forward (major to minor) rate constants of 25, 9.5, and 3.5 s^{-1}, leading to an estimated activation free energy near 11 kcal and an estimated activation enthalpy of 9 kcal.

Distance constraints derived from nuclear Overhauser enhancements were used for generating conformations of **1** for each of the states observed at 203 K. The distance geometry search procedure employed is described in Methods. The NOE-derived distances used are given in Table III. Additional backbone NOE's that might have been useful in defining conformation were not available because of overlaps with other NOE or exchange crosspeaks. Those distances listed, together with the anti (lower bound only) distance constraints chosen as described in Methods, provided information about the most probable conformations of the peptidic portion of the molecule, although they were insufficient to define the chirality of the disulfide bond. The clearest distinction in NOE's between the major and minor conformers at 203 K is in the estimated Asp H^{α}–mercaptoanilide H^{N} distance, which corresponds to the geometric maximum (3.6 Å) in the minor component and to near the minimum (2.2 Å) in the major component.

Quantitative use of the observed NOE data in this exchanging system may be questioned because of the possibility of magnetization transfer by exchange. The lifetime of the major component at 203 K (ca. 0.3 s) is comparable to the longer mixing times employed.[16] It was not possible to use lower temperatures to reduce the exchange rate further because of the rapid increase in viscosity of methanol below 200 K. However, as noted in Methods, only buildup curves which included 50, 100, and 150 ms points with good linear correlation were used for quantitative estimates of distances, and the resulting distance constraints for the major component should certainly be valid. The results for the minor component are more problematic, because its lifetime is 4 times shorter. Examination of the relative buildup rates of $A_{maj}X_{maj}$, $A_{min}X_{min}$, $A_{min}X_{maj}$, and $A_{maj}X_{min}$ crosspeaks suggests that, in the worst case, which is the Asp H^{α}–mercaptoanilide H^{N} crosspeak from the minor component, the volume buildup rate could be too small by a factor of 2, so that corresponding estimated distance constraint might be 12% too high. For peaks involving the major component, the error is not more than 2%. Given the −10% and +15% ranges applied to the NOE-derived distances, this component of magnetization transfer should not affect the outcome of the distance geometry searches or vitiate the conclusions drawn from them.

Within the 5-kcal total energy and 1.5-kcal constraint violation energy limits adopted, the constrained distance geometry search returned two classes of conformations for the *N*-MeArg-Gly-Asp moiety of the major component in methanol at 203 K. These could be subdivided on the basis of S–S bond chirality. Dihedral angles and calculated energies for the lowest energy conformations of each subclass are reported in Table IV. The conformations of class 1A±, which have the lowest total energy and near-zero constraint violation, were also those most frequently generated, and they included the 25 lowest energy structures of the 55 within the energy limits. They are characterized by an extended conformation (Φ, $\Psi \approx 180°, -150°$) at Gly and a C_7 like conformation (Φ, $\Psi \approx -80°, 80°$) at Asp. Like all of the other low-energy conformations to be described, these structures contain a trans benzoyl–*N*-MeArg peptide bond. The subset with positive disulfide chirality was the lower in energy and constraint violations (all members < 0.03 kcal) and included the 12 lowest energy conformations generated overall. Additionally, it may be noted that, although NOE data involving the Arg N^{α}-CH_3 of **1** were not used as input to the distance geometry calculations for lack of an internal H–CH_3 reference distance, a 2:1 ratio of the *N*-MeArg CH_3–mercaptobenzoyl H6 NOE to the *N*-MeArg CH_3–Arg H^{α} NOE was observed. This indicates that the former distance is 10–15% shorter than the latter and is consistent with a C6–C1–C7–N8 (See Figure 4 for numbering.) angle near −120°, as in 1A+, but not with an angle near −60°, as in 1A−. Conformation class 1A+ should therefore be considered to be the most likely conformation for the major component. Stereoviews of the overlaid backbones of the lowest energy exemplars with each disulfide chirality are shown in Figure 2.

The second set of *N*-MeArg-Gly-Asp conformations generated for the major component at 203 K, 1B±, also includes backbones with both disulfide chiralities. The subsets of both chiralities are higher in total energy and constraint energy violation than either subset of 1A and can therefore be deemed less probable. 1B± differs most importantly from 1A± in having a left-handed α-helical conformation (Φ, $\Psi \approx 60°, 60°$) at Asp, but the conformation at Gly is also less fully extended (α, $\Psi \approx 90°, 150°$). The helical arrangement at Asp defines a close approach to Asp H^{N} and mercaptoanilide H^{N} that produces the major violation of the NMR constraints. Because the r^{-6} dependence of Overhauser enhancements weights more heavily contributions from conformations with shorter interproton distances, this violation is a significant argument against the importance of 1B±. The minimum energy examples of 1B± are, however, given in Table IV, and overlays of the lowest energy exemplars are shown in Figure 2.

(15) Sandstrom, J. *Dynamic NMR Spectroscopy*; Academic Press Inc.: London, 1982; pp 6–18.

(16) Choe, B.; Cook, G. W.; Krishna, N. R. *J. Magn. Reson.* **1991**, *94*, 387–393.

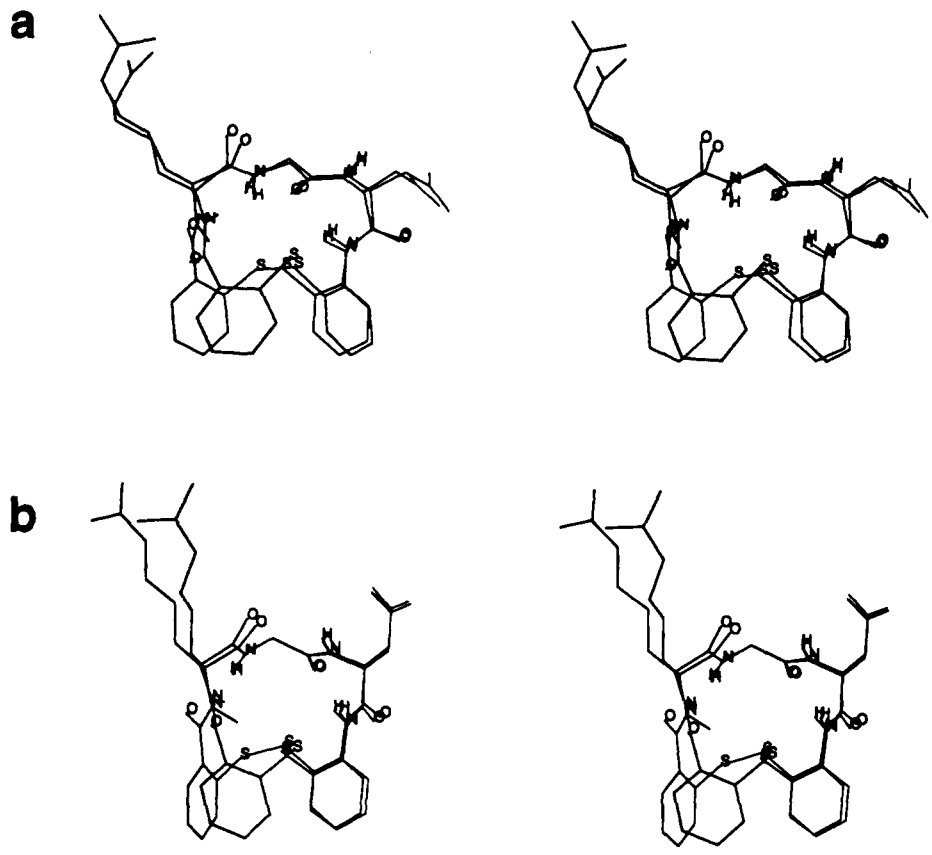

Figure 2. Stereoview of lowest energy exemplars of **1** (a) in conformations 1A+ and 1A− (both disulfide chiralities overlaid) and (b) in conformations 1B+ and 1B−. Conformation 1A+ (right handed −S−S chirality) represents the most probable conformation of the *N*-MeArg-Gly-Asp moiety of the major component in methanol at 203 K.

As mentioned, the chief spectroscopic difference between the major and minor conformers at 203 K is in the much weaker NOE involving the Asp H^{α} and mercaptoanilide H^{N} protons observed for the minor component. The conformations returned by the two searches therefore differ most clearly in the orientation of the Asp–mercaptoanilide amide plane relative to the overall ring. Three low-energy conformation classes were returned for the *N*-MeArg-Gly-Asp moiety of the minor component. One, 1C±, is characterized by an extended Gly residue ($\Phi, \Psi \approx 180, -150°$) and a right-handed α-helical conformation at Asp ($\Phi, \Psi \approx -70, -50°$), and another, 1D±, differs from 1C± by a 90° rotation of the Gly–Asp peptide bond plane. The two are of comparable total energy, and there is no obvious basis on the NMR evidence for judging one to be more probable than the other. In each case, both −S−S− chiralities are represented. The lowest energy exemplars are listed in Table IV, and overlays of the lowest energy exemplars are given in Figure 3. The third class, not shown and of higher total energy and constraint violation energy, also differs in the orientation of the Gly–Asp ring plane but may be excluded because it predicts a very strong Asp H^{N}–Asp H^{α} NOESY crosspeak, one corresponding to about 2.2 Å. Only a weak Asp H^{N}–Asp H^{α} crosspeak was observed, corresponding to an approximately 3.5-Å distance, but because the correlation coefficient for its buildup rate was less than 0.9, this datum was not used as quantitative input to the distance geometry search nor was it used as the basis for an ADC.

A 2:1 ratio of the Arg N^{α}-CH_3–mercaptobenzoyl Hδ NOE to the Arg N^{α}-CH_3–Arg H^{α} NOE was also observed for the minor component, again suggesting that the conformations with a C6–C1–C7–N8 angle near −120°, as in 1C+ and 1D+, are more likely.

To recapitulate, the major and minor components observed in methanol at 203 K differ most certainly in the orientation of the Asp–mercaptoanilide amide plane, and conformation 1A+ is the most probable for the *N*-MeArg-Gly-Asp moiety of the major component.

The data collected for **1** in 5:3 DMSO–sulfolane at 303 K are also given in Tables I and II. In light of the methanol solution results, it is probable that the room temperature DMSO–sulfolane data represent an average. However, if one class of conformation is dominant, the data may be expected to reflect that conformation. In fact, the class 1A+ conformation described above for the major component in methanol at 203 K is also the class of conformations of lowest energy found using the DMSO–sulfolane constraints. It has near-zero constraint violations, and 13 of the 15 lowest energy conformations returned by the search were members of it. To mark its similarity, the lowest energy exemplar is also listed in Table IV. Conformations with negative −S−S− chirality were also frequently returned, but the lowest energy version was 4.2 kcal above the lowest energy version with positive −S−S− chirality. A less likely class of *N*-MeArg-Gly-Asp conformations also returned by the search is marked by a rotation of the Gly–Asp peptide bond that brings the Asp H^{N} and Asp H^{α} into proximity. This proximity predicts a corresponding NOE buildup more than twice that observed and results in a nearly 1-kcal constraint energy violation.

Crystal Structure of 1. In the crystal, as in solution, **1** contains all trans peptide bonds (See Figure 4a.); the largest deviation, at the N^{α}-methylArg, is within 9° of the ideal 180° value. The *N*-MeArg-Gly-Asp region consists of a highly extended Gly residue ($\varphi, \Psi = -178°, -164°$) flanked by the N^{α}-methylArg residue in a conformation roughly consistent with an $i+2$ position of a β-turn ($\varphi, \Psi = -119°, 69°$) and an Asp residue in a conformation consistent with the $i+1$ residue of a Type I β-turn ($\varphi, \Psi = -61°, -33°$). The planes of the two aromatic rings are parallel, and the average plane of the extended *N*-MeArg-Gly-Asp backbone lies roughly perpendicular to them. This may be appreciated from the view provided in Figure 4b. All amide carbonyl oxygens extend outward and, with the exception of O10, are on one face of the ring.

The chirality of the disulfide bond is positive (C6–S1–S2–C23 torsion of 102°), consistent with results from the NMR and

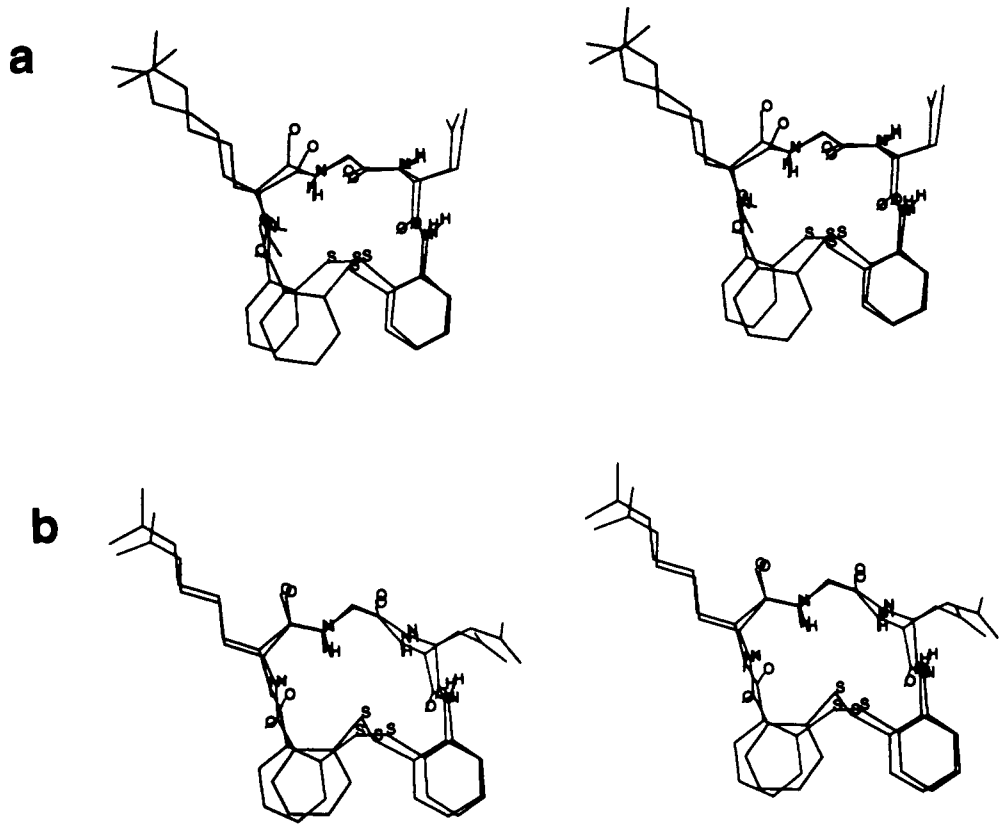

Figure 3. Stereoview of the lowest energy exemplars of the probable conformations of the minor component of **1** in methanol at 203 K. (a) Both chiralities of conformation 1C± overlaid. (b) Both chiralities of conformation 1D± overlaid.

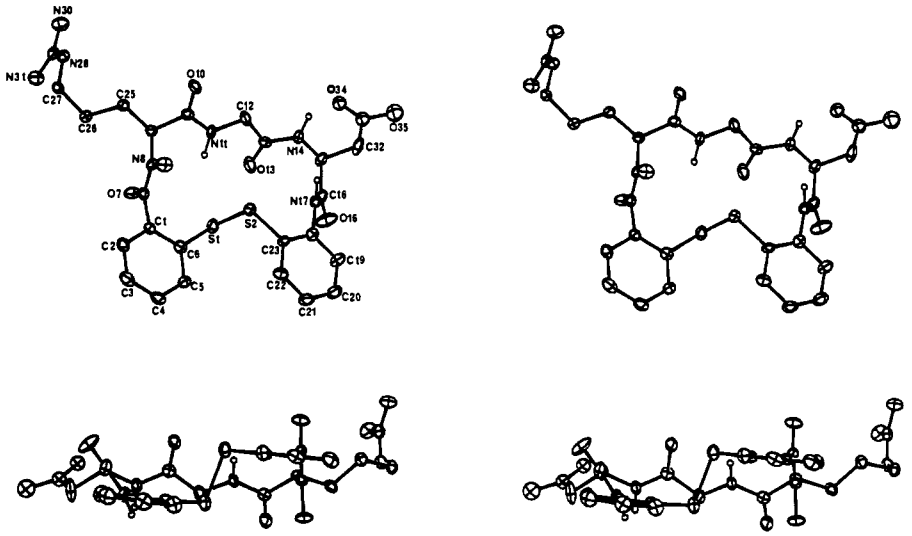

Figure 4. (a) Top: Stereoview of the crystal structure of **1**. Principal ellipses are drawn at the 50% probability level; H-atoms are small spheres of arbitrary size. Only one of the two aspartyl side-chain conformations is illustrated. (b) Bottom: Alternative stereoview looking into the mercaptobenzoyl, mercaptoanilide side of the cycle.

distance geometry analysis (vide supra) for conformer class 1C+ of the minor component in methanol solution. There is a remarkably close correspondence in individual backbone torsions between the crystal conformation and that likely conformation of the minor component in methanol. (See Table IV and Figure 5.)

Both side chains are extended away from the peptide backbone and do not appear to be involved in intramolecular H-bonds. The arginyl side chain adopts a partially extended conformation; principal torsion angles are $\chi^1 = -73°$, $\chi^2 = -171°$, $\chi^3 = 66°$, $\chi^4 = 80°$, $\chi^{5,1} = 3°$. The disordered aspartyl side chain adopts two conformations with $\chi^1 = -82°$ and $\chi^{2,1} = 17°$ for one orientation and $\chi^1 = -57°$ and $\chi^{2,1} = 38°$ for the second one.

Although the *N*-MeArg-Gly-Asp backbone conformation adopts a highly extended β-sheet type conformation in the crystal, the peptide groups do not participate in standard β-sheet type hydrogen bonding. Table V lists the hydrogen bonds involving backbone and side-chain groups. There are no transannular, intramolecular interactions observed. With the exception of the hydrogen at N11, all amide hydrogens participate in H-bonds between adjacent molecules of **1**. Given reasonable trigonal geometry, the only role for HN11 appears to be the formation of a possible intramolecular C_5 type structure with O13. All hydrogens from the protonated guanidinium and disordered aspartyl side chains also participate in the intermolecular H-bond network. In its 60% occupancy position, the Asp side-chain hydroxylic oxygen, O35, hydrogen

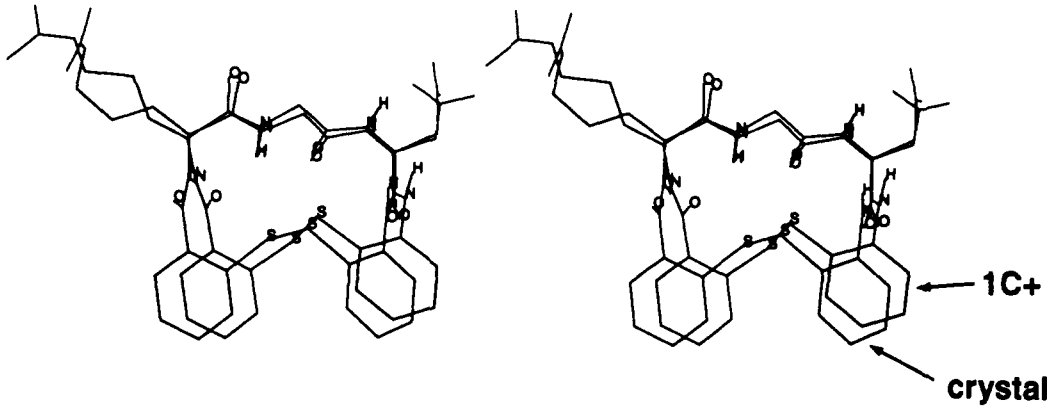

Figure 5. Stereo overlay of conformation 1C+ and the crystal structure of **1**.

Table V. Hydrogen Bonding Interactions in Crystal Structure of **1**[a]

donor	acceptor	distance, Å	angle, deg[b]	symmetry
N11	O13 (intra)	2.69	102	x, y, z
N14	O34	3.01	147[c]	$x-1, y, -z$
N14	O34′	2.96	151[c]	$x-1, y, -z$
N14	O7	2.83	175[c]	$x, y-1, z$
N17	O7	2.97	180	$x, y-1, z$
N28	O103	2.93	178	$^3/_2 - x, ^1/_2 + y, -z$
N30	O16	2.92	166	$1-x, y-1, -z$
N30	O104	2.82	175	$^3/_2 - x, ^1/_2 + y, -z$
N31	O10	2.86	168	$x, y+1, z$
N31	O1W	2.85	161	$^3/_2 - x, ^3/_2 + y, -z$
O35	O1W	2.63	172	$^1/_2 + x, y - ^1/_2, z$
O35′	O13	2.79	179	$x, y-1, z$
O1W	O13	3.02	178	$^1/_2 + x, ^1/_2 + y, z$
O1W	O101	2.55		x, y, z
O101	O104	2.97	178	x, y, z

[a] esd's of distances are at most 0.01 Å. [b] Angle at hydrogen. [c] See text for discussion of interactions involving N14.

bonds to the water molecule (O1W); in its 40% occupancy position, O35′ donates to amide oxygen O13. In both orientations, the carbonyl oxygen O34 appears to accept a hydrogen bond from N14. A short contact (2.83 Å) is noted between N14 and O7 for molecules related by translation along the *b*-axis, but the assumption of trigonal geometry at the nitrogen would preclude formation of a reasonably linear N14–O7 hydrogen bond. Distortion of angles at N14 to form the N14–O7 bond would in turn rule out the N14 hydrogen bonds to the aspartic acid side-chain carbonyl oxygen. The guanidinium group makes the ionic link to nitrate anion through interactions with two oxygens and also interacts with solvent molecules and peptide carbonyl groups. The tightest interactions in the crystal packing involve the arginyl and aspartyl side chains and the solvent water. Both the mercaptoanilide nitrogen, N17, and the Asp carbonyl oxygen, O16, are involved in the H-bonding scheme, but they each appear to participate in only one interaction. The effect of several H-bonds combined to glycyl carbonyl oxygen O13, from the water solvent, (partially) from the Asp side chain, and intramolecularly from N11 (C_5 structure) may be suggested as one possible cause for preference of this class 1C+ type conformation in the crystal over the predicted C_7 structure at Asp for the major solution class 1A± conformers.

Solution Conformations of 2. Ac-Cys-*N*-MeArg-Gly-Asp-Pen-NH_2 cyclic disulfide (**2**) gives single-component, narrow-line spectra at room temperature in methanol or DMSO–sulfolane, but low-temperature spectra in methanol (Figure 6) reveal the differential line broadening produced by conformational exchange. Separate components in slow exchange, however, are not observed down to 193 K for **2** in methanol. NOE data were therefore collected only for 5:3 DMSO–sulfolane solution at room temperature, with the hope that a dominant conformation would be indicated. Chemical shift and coupling constant data are given in Table II, and the distances derived from NOE buildup rates are merged in Table III with those from **1**. Because the chemical

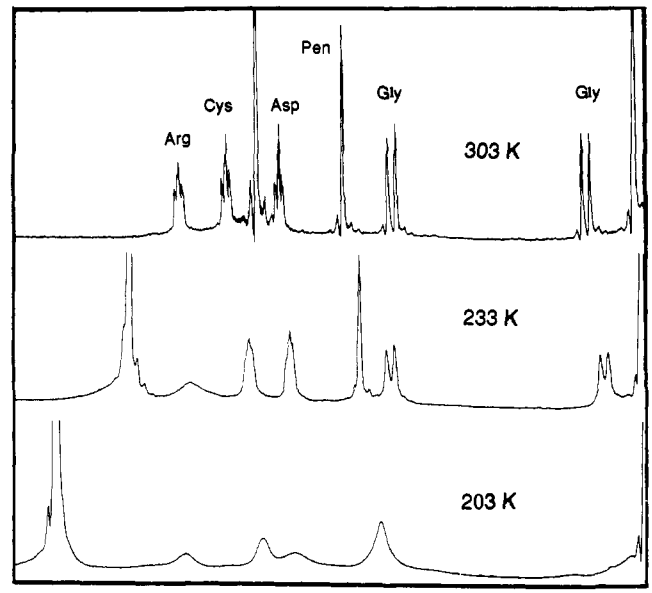

Figure 6. α-Proton resonances of **2** in methanol-d_4 at various temperatures. Differential line broadening is apparent, but separate forms in slow exchange were not observed down to 193 K.

shifts of the Pen β-CH_3 resonances were degenerate, and the closely spaced Cys H^β resonances overlapped the *N*-MeArg *N*-CH_3 resonance, no doubly-bounded NMR constraints could be set on the Cys-Pen side-chain portion of the cyclic structure.

For the *N*-MeArg-Gly-Asp moiety, the constrained distance geometry search returned 78 structures within 5 kcal in total energy of the lowest. These contained only trans peptide bonds. Two classes of low-energy conformations completely satisfied the NOE constraints used, showing constraint violation totals less than 0.1 kcal, and two additional classes were also of low energy but showed somewhat higher constraint violations. The dihedral angles at the four peptide bonds for the lowest energy exemplars of these four classes are given in Table VI.

The conformations of class 2A are distinguished by an extended conformation at Gly and an approximately C_7 conformation at Asp. They are analogous to the conformations considered most probable for the major component of **1** (Class 1A) and accounted for just under half of the low-energy conformations returned by the search. However, with the −10% and +15% distance bounds employed and the conservative lower distance limit, 3.0 Å, used as an ADC, the NMR observations for **2** are about as well accommodated by conformations of class 2B, in which the Gly residue is not extended. Such structures accounted for another quarter of the total, and there is no basis for ruling them unlikely. Conformations of class 2C, which have higher constraint violations, are similar to the class 1B conformations found for **1**. They have a left-handed α-helical conformation at Asp. This conformation at Asp may be judged to be unlikely in actuality because of the

Table VI. Possible Conformations of RGD Portion of Ac-Cys-N^{α}-MeArg-Gly-Asp-Pen-NH_2 Cyclic Disulfide (**2**) in DMSO–Sulfolane[a]

class	E_{total}[b], kcal mol^{-1}	E_{constr}, kcal mol^{-1}	ψ, deg	*N*-MeArg ϕ, deg	*N*-MeArg ψ, deg	Gly ϕ, deg	Gly ψ, deg	Asp ϕ, deg	Asp ψ, deg	ϕ, deg
2A	8.49	0.03	99	−124	68	−177	−161	−81	68	−135
2B	9.79	0.09	134	−107	110	78	−133	−63	142	−110
2C[c]	8.97	0.25	135	−115	64	82	146	53	74	−76
2D[c]	8.41[d]	0.50	72	51	63	74	−141	−93	146	−131

[a] RGD conformations of lowest energy member of each class returned by the constrained distance geometry searches. [b] Energy calculated by AMBER, not referred to a particular structure. [c] These conformations, although returned by the search, are judged unlikely because of the complete absence of certain NOE's. See text. [d] Global minimum of the 500 structures generated.

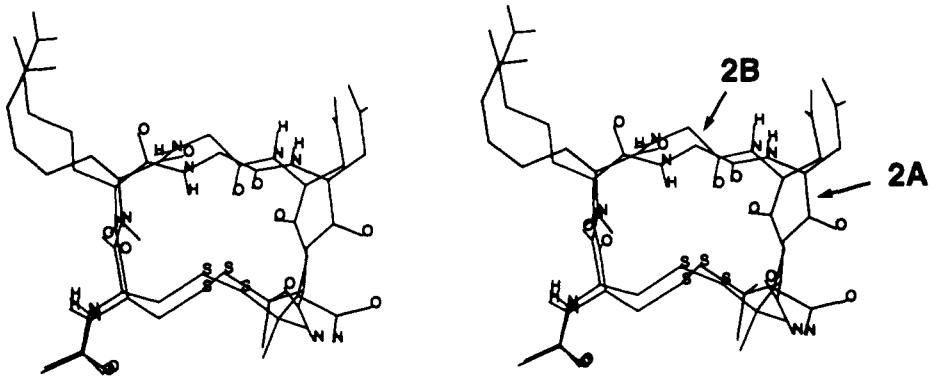

Figure 7. Stereo overlay of lowest energy exemplars of conformations consistent with the NOE observations of **2** in DMSO–sulfolane, conformations 2A and 2B. Gly H–N–C–H coupling constants suggest that 2A may be preferred.

absence of any observable Asp H^N–Pen H^N NOE; the helical arrangement requires a 2.5–3.5-Å separation. Conformations of class 2D, which have *N*-MeArg in the left-handed α-helical arrangement, should likewise be considered unlikely contributors because of the absence of an observable Gly H^N to *N*-MeArg CH_3 crosspeak. The helical arrangement would again require 2.5–3.5 Å, but from the acetyl CH_3–Cys H^N reference NOE, the lower bound for an unobserved peak may be estimated at >4 Å.

As might be expected, because the dialkyl disulfide **2** has two more internal torsional degrees of freedom than the diaryl disulfide **1**, the conformation of the former in solution is not so well defined, even by comparison with **1** at room temperature. The observations, made on what is certainly a rapidly exchanging mixture of conformations are consistent with conformations of both class 2A, with the extended Gly residue that appears to be dominant in **1**, and class 2B, in which the glycine residue is somewhat more bent. Figure 7 shows overlays of the lowest energy structures of the two most probable classes of conformation.

Discussion

The peptides studied in this work are among the most active non-protein Arg-Gly-Asp antagonists to the blood platelet GPIIb/IIIa receptor, and because of their cyclic structure, the Arg-Gly-Asp sequence in them is to a certain extent conformationally restricted. Potentially, therefore, they offer some of the information necessary for mapping the bound conformation of that sequence to support rational design of non-peptide mimetics. In spite of its polarity, which militates against peptide crystallization, we were fortunate in obtaining crystals of a salt of **1** (2-mercaptobenzoyl)-*N*-MeArg-Gly-Asp-2-mercaptoanilide cyclic disulfide) suitable for X-ray diffractometry. The crystal structure of **1** reported here exhibits a highly extended Gly residue flanked by an *N*-MeArg residue in a conformation roughly consistent with the $i+2$ position of a β-turn and an Asp residue in a conformation consistent with the $i+1$ position of a β-turn. We have dubbed this arrangement the "turn-extended-turn" conformation. Crystal structures of oligopeptides like this one are undoubtedly stable, low-energy conformations but, like solution structures, are not necessarily the receptor-bound conformations. Internal mobility of **1**, and thus the existence of other low-energy conformations, is clearly indicated by its NMR spectra, which at readily accessible temperatures reveal at least two conformational-exchange processes that can be brought into the intermediate rate range on the chemical shift time scale. One of these has an activation barrier of about 11 kcal and can be brought into slow exchange at or below 203 K; the barrier for the other is presumably higher, although only one of the components of the exchange is present in sufficiently high concentration to be detected directly. It is only reasonable to assume that there are other conformation-exchange processes, involving the backbone, as well as, of course, side-chain motions, that have barriers lower than 11 kcal and are in fast exchange at the lowest temperatures studied. Conclusions based on the NMR data are therefore realistic only in so far as they can be credited with reflecting a dominant conformation, or fit by a model involving (probably no more than two) exchanging conformations. In the case of **1** in DMSO–sulfolane at room temperature, the peptide is almost certainly exchanging at least between the two conformations that can be brought into slow exchange in methanol at 203 K. We have found that the most probable dominant conformation reflected by the room temperature NOE data is like the most probable conformation of the species that is observed to constitute 80% of the mixture at 203 K.

The turn-extended-turn Arg-Gly-Asp motif occurs not only in the crystal structure, but also in the structure that best fits the solution data for the major species of **1** observed at 203 K, and it also appears in one of the two classes of structure consistent with the observations for the minor component. Although the C_7 conformation at Asp in the major component at 203 K approximates that for the $i+1$ position of a Type II turn, the conformation at Asp in the crystal, and in the model of the minor component similar to it, approximates that for the $i+1$ position of a Type I turn.

It is of interest to speculate on the nature of the barrier between the two components observed at low temperature in methanol. Reference to Table IV and to Figures 2 and 3 would suggest that the difference between 1A+, the most likely conformation of the major component, and 1C+, the minor component conformation most nearly resembling the crystal structure, or the crystal structure itself lies in the orientation of the Asp–mercaptoanilide amide bond. The intrinsic barriers to rotation about the C^{α}–C' bond (Ψ) of a peptide[17] and about the aryl-N bond of an anilide[18] are low and will not account for the 11-kcal barrier estimated from

(17) Momany, F. A.; McGuire, R. F.; Burgess, A. W.; Scheraga, H. A. *J. Phys. Chem.* **1975**, *79*, 2361–2381.

the NMR spectra. (The ca. ±90° values in Table IV for the C16–N17–C18–C23 angle at Asp–mercaptoanilide are in fact near a predicted torsional maximum of ca. 3 kcal.[18]) Torsional barriers for disulfides, 7–9 kcal,[19-21] more nearly approach the observed barrier to exchange. However, a change in disulfide chirality need not be associated with the major–minor transition. The crystal structure and the lowest energy and most probable conformers of the major component both have positive –S–S– chirality, and the conformational searches indicate that in any case low-energy conformations with either disulfide chirality are possible for either orientation of the Asp–mercaptoanilide bond. It may be that rotation of the Asp–mercaptoanilide amide plane through the average ring plane requires a significant departure of the disulfide dihedral angle from the minima near ±90° to avoid bad van der Waals contacts in the process, but the strain need not be localized to this one bond. An analogous system in which significant strain is induced in the path of an amide plane rotation has been reported for cyclo(Pro-Gly)$_2$, for which NMR observations indicate a barrier of 13 kcal.[22]

In summary, for (2-mercaptobenzoyl)-*N*-MeArg-Gly-Asp-2-mercaptoanilide cyclic disulfide (**1**) the NMR data point with little ambiguity to the turn-extended-turn conformation 1A± for the *N*-MeArg-Gly-Asp region of the major component, and for the minor component, the data are consistent with the somewhat different (at Asp–mercaptoanilide) turn-extended-turn conformation found in the crystal. The less constrained heterodetic peptide Ac-Cys-*N*-MeArg-Gly-Asp-Pen-NH_2 cyclic disulfide (**2**) may have a dominant Arg-Gly-Asp conformation analogous to that of the major component of **1**, but conformations less extended at the glycine residue cannot be excluded. The degenerate chemical shifts of the Pen β-CH_3 resonances and the small separation of the Cys β-protons (0.09 ppm) do tend to suggest that the $C^{\beta}H_2$–$C^{\beta}(CH_3)_2$ portion of the ring of **2** is not very constrained. On the other hand, the 0.76 ppm splitting of the Gly α-protons, while hardly the largest backbone methylene splitting observed in cyclic peptides (For example, the Gly H^{α} in cyclo(Gly-Sar)$_2$ are split by 1.35 ppm.[23]), does suggest that there is perhaps some conformational preference at that residue. Although the H^N–H^{α} NOE data do not distinguish them, the H^N–H^{α} couplings,[24] at Gly, 7.3 and 3.6 Hz, are arguably more consistent with Φ_{Gly} on one side or the other of 180°, as in the turn-extended turn conformation 2A, than with a value near 80°, as in the other conformations listed in Table VI.

Conformational studies have been reported for Boc-Cys-Ala-Aib-Gly-Cys-NHMe disulfide, an analog of the same ring type as **2**.[25] For that molecule, a conformation with a C_7 arrangement at Aib and an antiparallel β pairing of the Cys-Ala and Gly-Cys sequences is only tentatively suggested, on the basis of N–H solvent exposure data, steady state NOE's, and modeling. That proposed conformation involves an $N—H_{Ala}\cdots O{=}C_{Gly}$ hydrogen bond. Conformations like it would be less likely in the case of **2**, in which the corresponding N–H is replaced by N–Me. In any event, examination of the distance geometry search output for **2** shows that analogous structures are unlikely for **2**. Conformations in which the Gly residue approaches the C_7 regions of the Ramachandran map (or the α regions, which could yield a similar ring shape) occur only at high energy (>10 kcal in nonbonded energy) and with significant NOE constraint violations (>1.8 kcal).

More recently, Bogusky et al.[26] have reported on two much closer analogs of **2**, Ac-Cys-Arg-Gly-Asp-Cys-NH_2 disulfide (**3**) and Ac-Cys-Arg-Gly-D-Asp-Cys-NH_2 disulfide (**4**), studied in DMSO solution. They were unable to find single conformations of these molecules consistent with all of their NOE observations and instead described pairs of conformers that could, in equimolar ratio, predict their observations. In both cases, one member of the pair did contain an extended Gly residue. For **1** and **2**, on the other hand, we were able to find conformations that satisfied our NOE data and were consistent with the H–N–C–H coupling information, without constraint violations. In particular, Bogusky et al. observed for the all-L isomer H^N_{Arg}–H^N_{Gly}, H^N_{Gly}–H^N_{Asp}, H^N_{Asp}–H^N_{Cys2}, and H^N_{Arg}–H^N_{Asp} NOE's, the equivalents of which were not observed by us and for which we assigned 3-Å ADC's. The differing observations could be a result of differing conditions: They used data out to 500-ms mixing time; we collected data only to 150 ms, although we used a more viscous solvent mixture. However, we believe it more likely that the difference is constitutional, that **2**, by virtue of the penicillamine (β,β-dimethyl-Cys) substitution and the additional N^{α}-methyl group[27] at Arg, is conformationally more constrained. In the course of this work, we also examined Ac-Cys-D-Arg-Gly-Asp-Pen-NH_2 (**5**), which lacks the N^{α}-methyl group and did find, in agreement with the reported results on **3**, that the NOE observations, which in that case included the vicinal H^N–H^N NOE's reported for **3**, are quantitatively inconsistent with a single conformation.[28]

In an earlier paper,[6] we showed that the use of conservatively chosen lower distance bounds for unobserved NOE's, so-called ADC's, reduced the number of outlying structures generated by the distance geometry search procedure. In the present work, as before, we used a 3.0-Å lower bound for the anti distance constraints in the distance geometry input, although, depending on the noise in the particular region of the NOESY spectra, the adjacency of other crosspeaks, the concentration of the species examined, and other factors, there were certainly instances in which greater lower bounds for the ADC's, e.g., 3.5 Å, could have safely been employed. On the other hand, there were also instances in which lower bounds greater than 3.0 Å would have been inappropriate. As indicated in Methods, we omitted constraints entirely when in doubt. Because the ADC's far outnumber the experimental NOE's, we performed a control calculation using ADC's only for the major component of **1**. The resulting distribution of dihedral angles was different and much less exclusive than the distribution obtained when the observed NOE data are included. The ADC's alone do not narrowly restrict the ring conformations.

A final comment should be made. We have proposed two likely conformations for **1**, a somewhat conformationally restricted, but highly active antagonist of the platelet GPIIb/IIIa receptor. It is obviously not possible to state which, if either, of these conformations corresponds to the receptor-bound state of this antagonist, since they differ little in energy and are in equilibrium. Synthesis and testing of additional, differently constrained, Arg-Gly-Asp analogs are required to refine the picture of the receptor-bound state.

Acknowledgment. We thank Dr. Fadia E. Ali and Dr. James M. Samanen for the peptides studied in this work.

Supplementary Material Available: Tables of atom coordinates, anisotropic displacement parameters, and bond distances and angles (8 pages); listing of structure factors (18 pages). Ordering information is given on any current masthead page.

(18) Hummel, J. P.; Flory, P. J. *Macromolecules* **1980**, *13*, 479–484.
(19) Fraser, R. R.; Boussard, G.; Saunders, J. K.; Lambert, J. B.; Mixan, C. E. *J. Am. Chem. Soc.* **1971**, *93*, 3822–3823.
(20) Allinger, N. L.; Hickey, M. J.; Kao, J. *J. Am. Chem. Soc.* **1976**, *98*, 2741–2745.
(21) Khwaja, H. A.; Walker, S. *Z. Phys. Chem. (Munich)* **1987**, *153*, 151–160.
(22) Deber, C. M.; Fossel, E. T.; Blout, E. R. *J. Am. Chem. Soc.* **1974**, *96*, 4015–4017.
(23) Dale, J.; Titlestad, K. *Chem. Commun.* **1970**, 1403–1404.
(24) Pardi, A.; Billeter, M.; Wüthrich, K. *J. Mol. Biol.* **1984**, *180*, 741–751.
(25) Kishore, R.; Raghothama, S.; Balaram, P. *Int. J. Pept. Protein Res.* **1987**, *29*, 381–391.
(26) Bogusky, M. J.; Naylor, A. M.; Pitzenberger, S. M.; Nutt, R. F.; Brady, S. F.; Colton, C. D.; Sisko, J. T.; Anderson, P. S.; Veber, D. F. *Int. J. Pept. Protein Res.* **1992**, *39*, 63–76.
(27) Manavalan, P.; Momany, F. A. *Biopolymers* **1980**, *19*, 1943–1973.
(28) Unpublished work from this laboratory.